Available online at www.sciencedirect.com
ScienceDirect
Experimental Eye Research 85 (2007) 202–218
EXPERIMENTAL EYE RESEARCH
www.elsevier.com/locate/yexer

Age-related changes in human macular Bruch's membrane as seen by quick-freeze/deep-etch

Jiahn-Dar Huang [a], J. Brett Presley [b], Melissa F. Chimento [b], Christine A. Curcio [b], Mark Johnson [a,*]

[a] Department of Biomedical Engineering, Northwestern University, 2145 Sheridan Road, Evanston, IL 60208-3107, USA
[b] Department of Ophthalmology, University of Alabama School of Medicine, Birmingham, AL, USA

Received 31 January 2007; accepted in revised form 29 March 2007
Available online 3 May 2007

Abstract

Lipid-containing inclusions have been observed in human Bruch's membrane (BrM) and are postulated to be associated with age-related maculopathy (ARM), a major cause of legal blindness in developed countries. The dehydration associated with specimen preparation for thin-section transmission electron microscopy causes loss of these inclusions. Better preservation of the ultrastructure of the inclusions and tissue is achieved by using a quick-freeze/deep-etch preparation. We use this technique to examine normal human macular BrM in order to characterize the deposition of the lipid-rich inclusions and their age-related accumulation within different layers of the tissue. We find that various inclusions mentioned in other studies can be formed by combinations of three basic structures: lipoprotein-like particles (LLPs), small granules (SGs) and membrane-like structures. These inclusions are associated with collagen and elastic fibrils by fine filaments. In younger eyes, these inclusions are found mostly in the elastic (EL) and outer collageneous layer (OCL) and occupy a small fraction of the interfibrillar spacing. As age increases, LLPs and SGs gradually fill the interfibrillar spacing of the EL and inner collageneous layer (ICL) of the tissue, and later form a new sublayer, the lipid wall, within the boundary region between the basal lamina of retinal pigment epithelium (RPE) and ICL. Because the formation of the lipid wall only occurs after these inclusions fill the ICL, and it seems unlikely that the LLPs can pass through the packed layer, this result suggests a possible RPE origin of the LLPs that make up the lipid wall.
© 2007 Elsevier Ltd. All rights reserved.

Keywords: age-related maculopathy; age-related macular degeneration; Bruch's membrane; lipids; lipoproteins; electron microscopy; extracellular matrix; ultrastructures

1. Introduction

Bruch's membrane (BrM) is a thin layer of connective tissue located between the retinal pigment epithelium (RPE) and the choriocapillaris. Due to its specific location and properties, this tissue is thought to be a vital limiting layer for metabolic transport between the RPE cells and the choriocapillaris (Marshall et al., 1998). The RPE in turn plays an important role in the maintenance of photoreceptor metabolism (Kornzweig, 1977; Anderson et al., 1978; Matsumoto et al., 1987; Korte et al., 1989; Giusto et al., 1997). Compromise of the nutrient and waste transport through this region would eventually affect the photoreceptor's normal function and thus has been suggested as a possible cause of age-related maculopathy (ARM) (Sarks, 1976; Grindle and Marshall, 1978; Bird and Marshall, 1986; Chen et al., 1992; Starita et al., 1996), a leading cause of blindness in developed countries (Foster and Resnikoff, 2005). Age-related changes and accumulation of apparent "debris" in BrM are thought to compromise this transport (Killingsworth, 1987; Chen et al., 1992; Moore et al., 1995; Starita et al., 1996).

With advanced age, both the thickness and complexity of BrM increase primarily due to extracellular matrix remodeling and accumulation of inclusions in this region (Ramrattan et al.,

* Corresponding author. Tel.: +1 847 467 7143; fax: +1 847 491 4928.
E-mail address: m-johnson2@northwestern.edu (M. Johnson).

0014-4835/$ - see front matter © 2007 Elsevier Ltd. All rights reserved.
doi:10.1016/j.exer.2007.03.011

1994). These inclusions include advanced glycation endproducts (AGEs), coated vesicle-like bodies, spiked coated vesicle-like bodies, electron-lucent droplets, membranous debris, coated membrane-bound bodies (CMBBs), long spacing collagen and lipoprotein-like particles (LLPs) (Hogan and Alvarado, 1967; Grindle and Marshall, 1978; Feeney-Burns and Ellersieck, 1985; Killingsworth, 1987; van der Schaft et al., 1991; Handa et al., 1999; Ruberti et al., 2003; Li et al., 2005a; Yamada et al., 2006). In the later stage of human life, these inclusions presumably fuse or aggregate to form drusen and the basal deposits that are associated with age-related macular degeneration (Sarks, 1976; Pauleikhoff et al., 1990; van der Schaft et al., 1992; Green and Enger, 1993; Curcio and Millican, 1999). The accumulation of these inclusions may impede physiologic transport through this region (Hogan and Alvarado, 1967; Killingsworth, 1987; Curcio and Millican, 1999). The hydraulic conductivity, the permeability to macromolecular transport, and the elasticity of BrM are all found to decrease with advancing age (Moore et al., 1995; Starita et al., 1996; Hussain et al., 2002; Ugarte et al., 2006), and these events may disturb the metabolism of the RPE and photoreceptor cells.

In order to characterize these ultrastructural changes in BrM, studies using conventional thin-sectioning transmission electron microscopy (TEM) and histochemical methods have identified various inclusions and the age-related changes of the tissue (Nakaizumi et al., 1964; Feeney-Burns and Ellersieck, 1985; Killingsworth, 1987; Curcio et al., 2001). However, preparative steps for these procedures, such as the dehydration necessary for conventional TEM, result in ultrastructural loss and removal of lipids from the tissue (Guyton and Klemp, 1988; Overby et al., 2001; Ruberti et al., 2003). A better characterization of the accumulation of the lipid-rich inclusions, along with ultrastructural features and the consequent age-related changes of BrM, can provide valuable information related to the progression of accumulation of these inclusions and their influence on transport through this region.

Ruberti et al. (2003) used the quick-freeze/deep-etch (QFDE) technique to preserve lipids and to visualize the ultrastructural features within BrM. Their images of a small number of older eyes not only demonstrated lipid-rich particles accumulating in BrM, but also revealed the ''lipid wall'' that is formed by these particles in the inner ICL in some older eyes. In this study, we use this technique to examine normal human BrM in a larger series of eyes in order to characterize the progression of inclusion deposition and age-related ultrastructural changes of the extracellular compartment.

2. Methods

2.1. Eye tissues

Human eyes were obtained from Alabama Eye Bank within 4 h post-mortem. Eyes with drusen larger than 63 μm or any other grossly visible chorioretinal pathologic disturbance in the macula were excluded. Also, eyes from donors with diabetes or receiving artificial respiration longer than 5 days were excluded. Sixteen normal eyes were examined in this study, including two previously described eyes (Ruberti et al., 2003) (Table 1).

The posterior segment of the normal eyes was preserved by immersion in 0.1 M phosphate buffer solution with 2.5% glutaraldehyde and 1% paraformaldehyde for at least 24 h after the removal of the anterior segment. The macular region, including the retina, RPE, BrM, choroid, and sclera, was then dissected into 16 2 × 2 mm square blocks for QFDE or thin-sectioning TEM processing. A few of the tissue blocks were treated with Folch reagent (chloroform/methanol, 2:1) before QFDE processing to remove the lipids in BrM and see the effects on the ultrastructure.

2.2. QFDE processing

For eyes examined by QFDE, the retina layer was pulled away using fine forceps. The RPE–BrM–choroid–sclera complex was slam frozen in liquid nitrogen (−196 °C) in a Leica EM MM80E (Leica Microsystems Inc., Bannockburn, IL). The frozen tissue, with the RPE side facing up, was then transferred into a freeze-fracture deep-etch chamber (Cressington CFE-60, Cressington Scientific Instruments Ltd., Watford, UK) held at a vacuum level of 10^{-7} mbar. To reveal BrM, the tissue block was fractured obliquely by a cold razor blade and then etched at −95 °C for 25 min. After etching, a replica of exposed BrM ultrastructure was made by rotary shadowing using a platinum/carbon mixture at angle of 20° to the tissue surface and then further strengthened by coating with carbon from above. The replica was then immersed along with the tissue into a digestion solution (water/bleach, 1:1). The sclera was removed soon after the beginning of the immersion. The replica and the remaining chorioretinal juncture remained in the solution for at least 2 h to remove the tissue. The remaining replica pieces were then picked up by copper hexagonal grids, air dried, and examined using a JEOL-100 CX (JEOL USA, Peabody MA) electron microscope. Micrographs of the replica

Table 1
Sample eyes

Donor age	Gender	Ethnicity
27	F	AA
29	M	C
34	F	C
35	F	C
41	F	C
45	M	C
50	M	C
53	M	C
58	F	C
59	M	C
63	M	C
64	M	AA
77	F	C
78	M	C
80	M	C
82	F	C
86	M	AA

F, female; M, male; C, Caucasian; AA, African-American.

were scanned at 1500 lpi using an AGFA Duoscan T2500 (AGFA USA, Ridgefield Park NJ) in TIFF format and examined on a Power Mac G5 (Apple, Cupertino CA).

2.3. Thin-sectioning TEM

For each macula, 1–2 fixed tissue blocks were also post fixed using osmium–tannic acid–paraphenylenediamine (OTAP) to preserve neutral lipid components (Guyton and Klemp, 1988; Curcio et al., 2005a). Tissues were then dehydrated, infiltrated, and embedded in PolyBed 812 (Polysciences, Warrington, PA). One-micrometer thick sections were stained with 1% toluidine-blue-O in 2% sodium borohydrate. Thin sections were examined using a JEOL1200 EXII (JEOL USA, Peabody, MA) or a Hitachi 7000 (Hitachi High Technology America, Pleasanton, CA) electron microscope. Representative negatives of thin sections (Kodak EM film 4489) were scanned with a PowerLook 1100 scanner and Umax Magiscan 4.5 (Umax Technologies Inc., Dallas, TX).

3. Results

The five layers of BrM lying between the RPE and the fenestrated choriocapillaris, when examined using QFDE, could be distinguished by their morphological features (Fig. 1). The layers are not always continuous across the images. On both aspects of the tissue resided two thin layers of tight meshwork, the basal lamina of the RPE (BL-RPE) (Fig. 2A) and the basal lamina of the choriocapillaris (BL-CC) (Fig. 2D). The smooth and wide band-like material seen in the center of BrM were elastic fibrils that clearly marked the location of the elastic layer (EL) (Fig. 2C). Separated by the EL, the inner collageneous layer (ICL) (Fig. 2B) and the outer collageneous layer (OCL) (Fig. 2D) were fibril networks located on the RPE and choriocapillaris side, respectively. The ICL, EL, and OCL were defined as middle layers of BrM in this study. The EL was not always apparent in QFDE replicas.

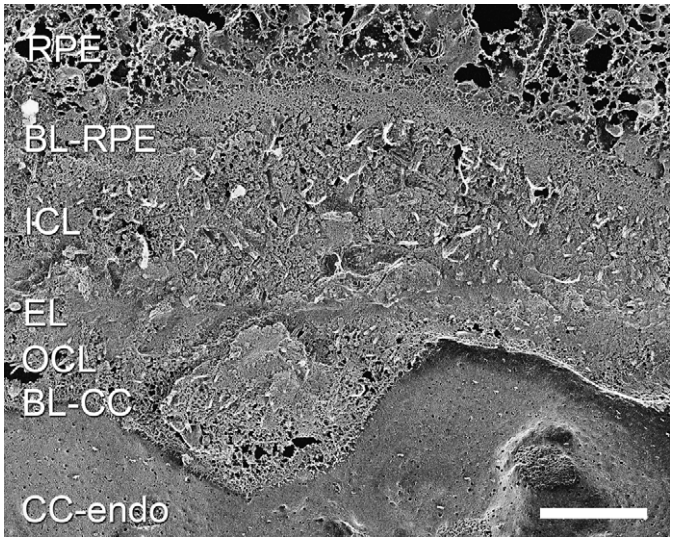

Fig. 1. An oblique QFDE section of the RPE-BrM-choriocapillaris complex of a 45-year-old eye. Different layers of BrM are: RPE, retinal pigment epithelium; BL-RPE, basal lamina of the RPE; ICL, inner collageneous layer; EL, elastic layer; OCL, outer collageneous layer; BL-CC, basal lamina of choriocapillaris; and CC-endo, choriocapillaris endothelium marked in the figure. Bar 2 μm.

The collagen fibrils seen in the middle layers occasionally showed 64 nm periodicity. The fine preservation of the tissue using the QFDE method demonstrated exquisite ultrastructures of the extracellular components and the associations among them. The age of eyes used in this study covered from the 3rd to the 9th decade of human life allowing us to investigate the age-related changes of these ultrastructures within different layers of the tissue.

3.1. Inclusions seen in BrM using QFDE

Different inclusions were observed in BrM even in the youngest eyes examined. We found three basic types of inclusions in QFDE images: lipoprotein-like particles (LLPs), small granules (SGs), and the membrane-like structures that formed coated membrane-bound bodies (CMBBs) when combined with LLPs and SGs. These inclusions were usually found in the middle three layers of BrM.

LLPs were one of the major materials that accumulated with age in BrM (Fig. 3A). As we reported previously (Ruberti et al., 2003), these spheroids appeared as a concentric core-shell ultrastructure. LLPs were identified as lipid containing based on several characteristics. First, they appeared solid and did not etch significantly during the QFDE process, indicating that they contained only little water. Second, their morphological appearance was similar to that reported in studies of low-density lipoproteins that accumulate in intima observed by QFDE (Frank and Fogelman, 1989). Third, they appeared in the same locations in BrM as LLPs have been found using other lipid preserving techniques (Curcio et al., 2001; Ruberti et al., 2003). Finally, these particles were extracted from the QFDE images when the tissue was pretreated with Folch reagent to remove lipids (Huang, 2007). The size of the LLPs usually varied from 60 to 100 nm but sometimes could be as large as 300 nm. Large LLPs were probably formed by the fusion of two or more individual LLPs as shown in Fig. 3B. The LLPs were frequently seen in contact with fine filaments (Fig. 4A), presumably proteoglycans that extended among collagen and elastic fibrils. In addition, the LLPs were found associated with SGs, as described below (Fig. 4B).

A large number of SGs were observed in the middle layers of BrM. They appeared as small round particles of approximately 10 nm in diameter with no other obvious morphological characteristics (Fig. 5A). Similar to the LLPs, the SGs also were attached to the fine filaments (Fig. 5B). Sometimes clusters of the tightly packed SGs were found in the tissue (Fig. 5C).

An interesting morphological feature was the complex composed by a single LLP and one or more layers of surrounding SGs. Variability in the fracture plane passively around an LLP allowed us to infer the ultrastructure of this complex, as seen in Fig. 6. Since the size of the LLP and the number of layers of the SGs varied from one LLP to another, the size of the complex varied from about 100 nm to 300 nm. Short struts

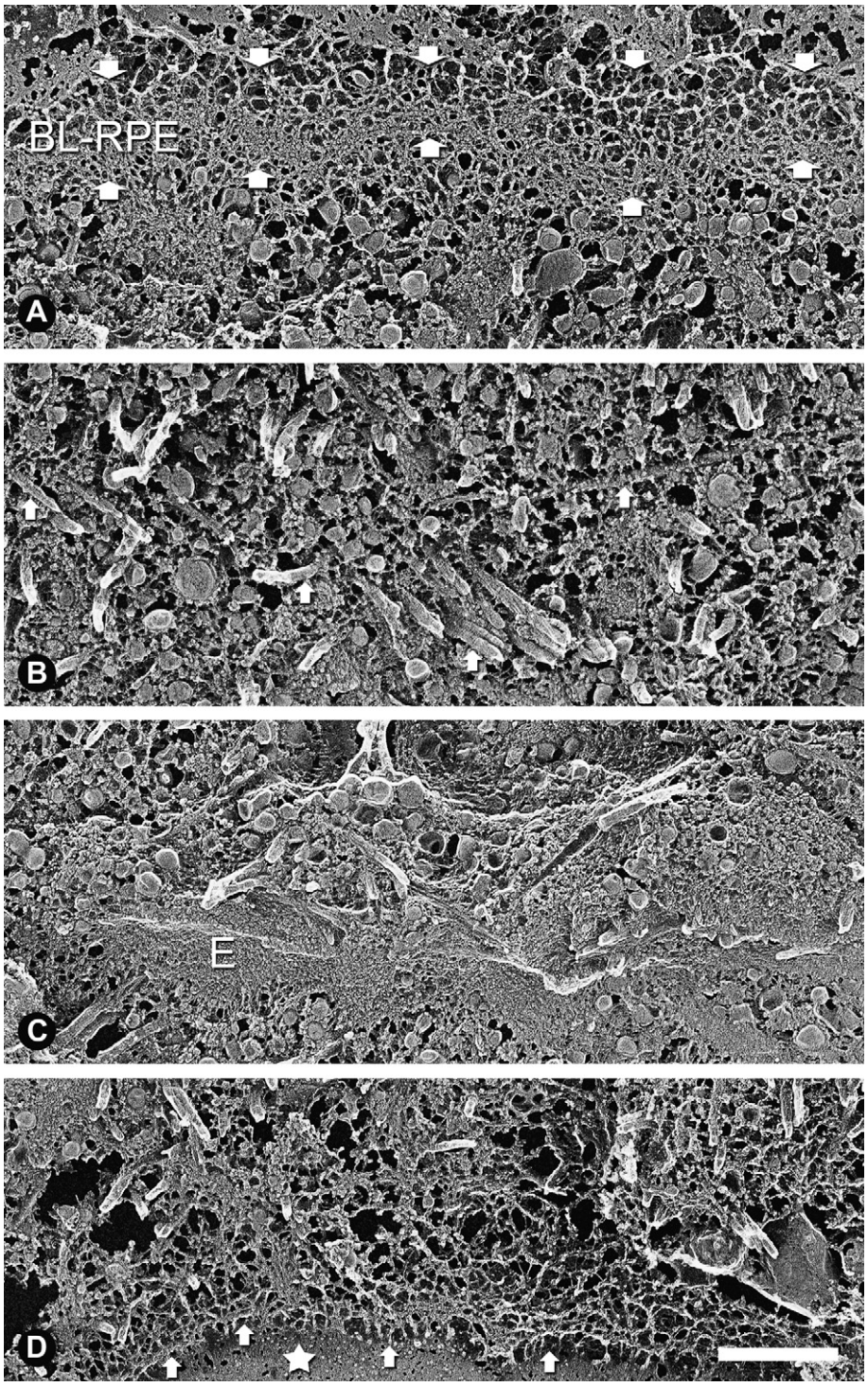

Fig. 2. Higher magnification images of different layers of the oblique section seen in Fig. 1. (A) The basal lamina of RPE cells. Notice that the BL-RPE was divided into two sublayers. On the RPE side was the lamina lucida and on the other side was the lamina densa. Arrows indicate the boundary of the BL-RPE. (B) The ICL was composed of collagen fibrils (arrows) and fine filaments, on which the lipoprotein-like particles (LLPs) and small granules (SGs) were accumulated. (C) EL was marked by the wide, smooth elastin fibrils. This layer also contained the collagen fibrils and fine filaments. E, the elastin fibrils. (D) The OCL and the thin BL-CC. The OCL was composed of the same components as the ICL. The thin layer of BL-CC, indicated by arrows, was located adjacent to the vessel wall of choriocapillaris. Star, the vessel wall of choriocapillaris. Bar 500 nm.

were found radiating from the SG layer and associating with nearby fibrils.

The CMBB was a more complicated configuration that was composed of LLPs and SGs, absent the collagen fibrils, surrounded by a membrane-like structure (Fig. 7A). The membrane-like structure, about 15 nm wide and sometimes double-layered, showed a granular appearance and formed either a closed or opened loop (Fig. 7B). Within the loop, the LLPs

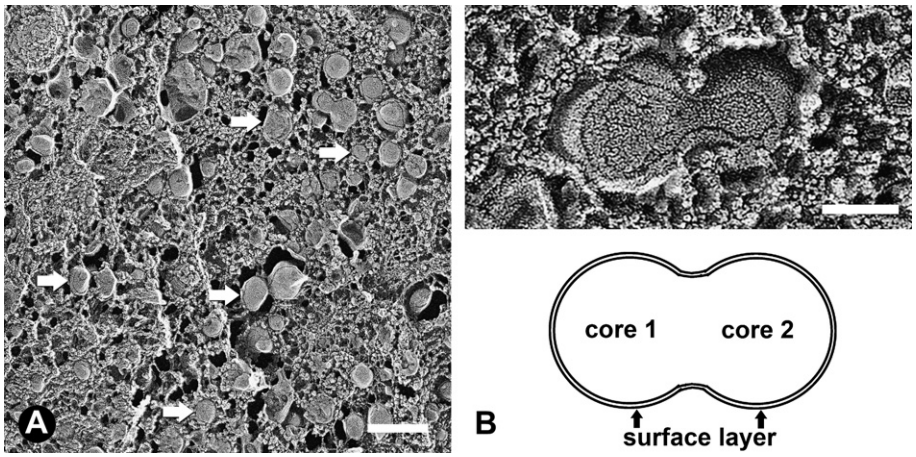

Fig. 3. (A) LLPs (arrows) were the major inclusions seen in BrM of a 45-year-old eye. The particle was usually 60–100 nm in diameter and composed of a core surrounded by a thin surface layer. Bar 200 nm. (B) Two LLPs fused to form a dumbbell-shaped particle in a 78-year-old eye. Bar 50 nm.

and SGs were packed with short thin filaments associated with these inclusions. Sometimes the LLP–SG complexes described above were also found in the loop. Outside the loop, short struts stretched out from the membrane-like structure and connected to nearby fibrils (Fig. 7B). The CMBBs were seen in both collageneous layers and in the EL of BrM.

Different types of small drusenoid structures, clearly visible in eyes prepared by OTAP (Fig. 8), were also identified by QFDE (Fig. 9). High magnification QFDE images showed that these structures contained all the inclusions just described (Fig. 10A). Tightly packed within the drusenoid structure, the inclusions were occasionally seen to be associated with short, thin filaments. The CMBBs seemed to be the major component, with these structures found everywhere. We found no collagen fibrils from the collageneous layer within the drusenoid structures (Fig. 10B). A thin layer of BL-RPE separated them from the RPE cells. Fine fibrils were seen extending from the lamina densa into the drusenoid structures and associating with its components (Fig. 10C).

The long spacing collagen, described in other morphological studies of BrM (Hogan and Alvarado, 1967; Grindle and Marshall, 1978; Killingsworth, 1987; Newsome et al., 1987), was not identified in our QFDE preparations. In our study, long spacing collagen was observed only when examining the tissues using OTAP thin-sectioning TEM (data not shown). In OTAP images, the long spacing collagens found in BrM demonstrated morphological features similar to those previously described in other studies (Grindle and Marshall, 1978; Newsome et al., 1987).

It appeared that with increased donor age, BrM became more packed with these inclusions with a concomitant reduction of intervening void space. A closer examination indicated that the major accumulated inclusions are LLPs and SGs. We also found the filling of the tissue was not homogeneously distributed in all layers, as described below.

3.2. Progression of LLP and SG deposition and the formation of the lipid wall

With advanced donor age, an increased deposition of LLPs and SGs in BrM was seen that gradually filled the tissue. A progression of the inclusion accumulation was observed. In eyes <40 years, the EL and OCL seemed to be more filled than the ICL and the inclusions were mostly found in these

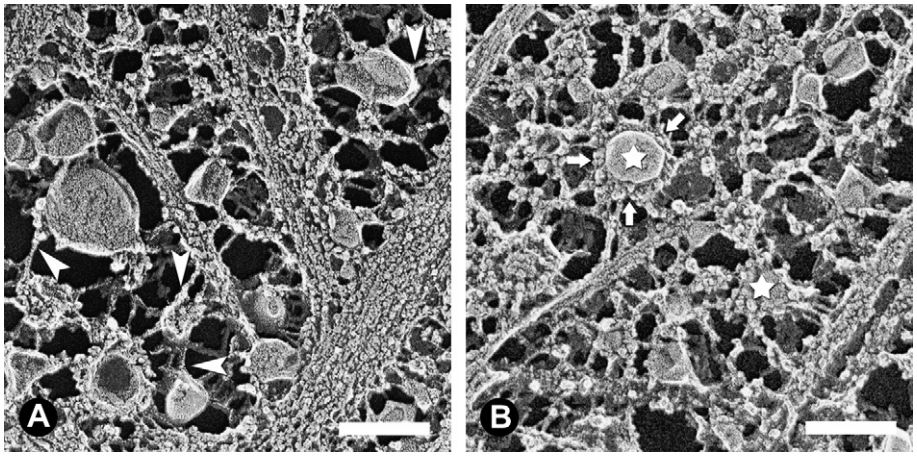

Fig. 4. (A) LLPs were associated with fine filaments as indicated by arrowheads. Eye, 34 years. Bar 150 nm. (B) SGs (arrows) surrounded the LLPs (stars). Bar 150 nm.

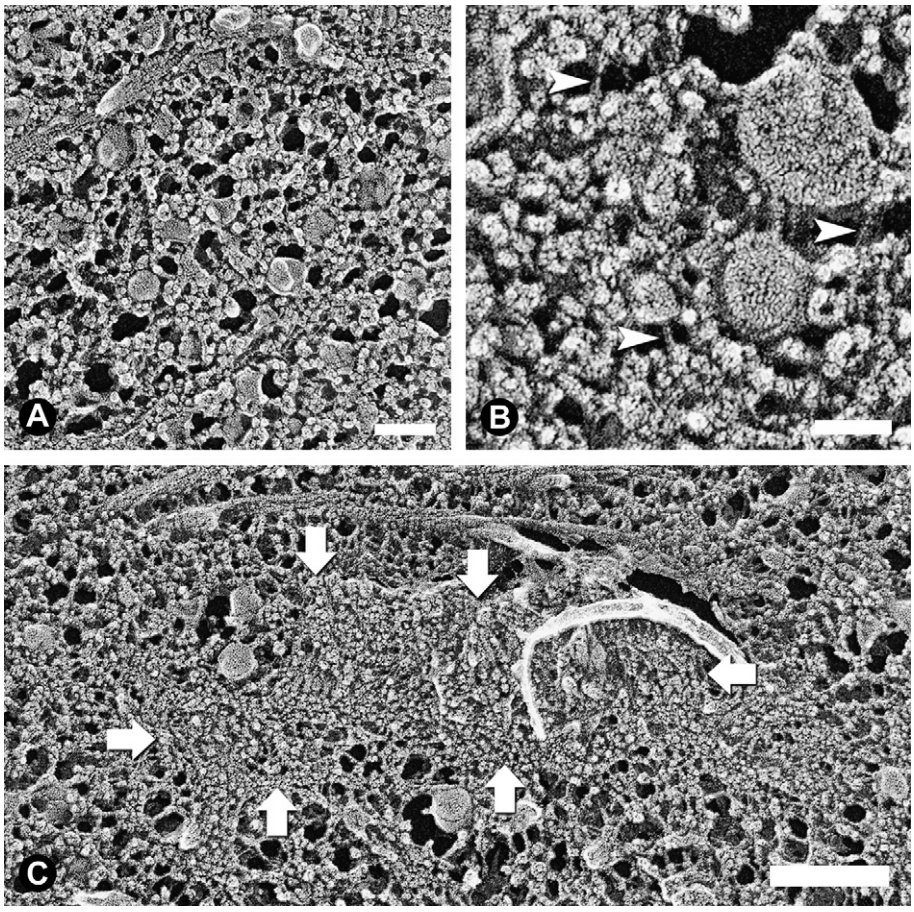

Fig. 5. (A) SGs were small round solid particles deposited among LLPs. Eye, 29 years. Bar 50 nm. (B) They were usually seen attached to the fine filaments (arrowheads) or LLPs in the tissue. Eye, 34 years. Bar 25 nm. (C) Cluster of tightly packed SGs (arrows) were also observed. Eye, 34 years. Bar 200 nm.

two layers (Fig. 11A). With increasing age, both EL and ICL showed significant amounts of the inclusions, and thus appeared more crowded than did the OCL in old eyes (Fig. 11B). The inclusions were rarely found inside either the BL-RPE or the BL-CC in any samples of our study (data not shown).

Although inclusions were usually found in the OCL, their number did not appear to increase with aging (Fig. 12).

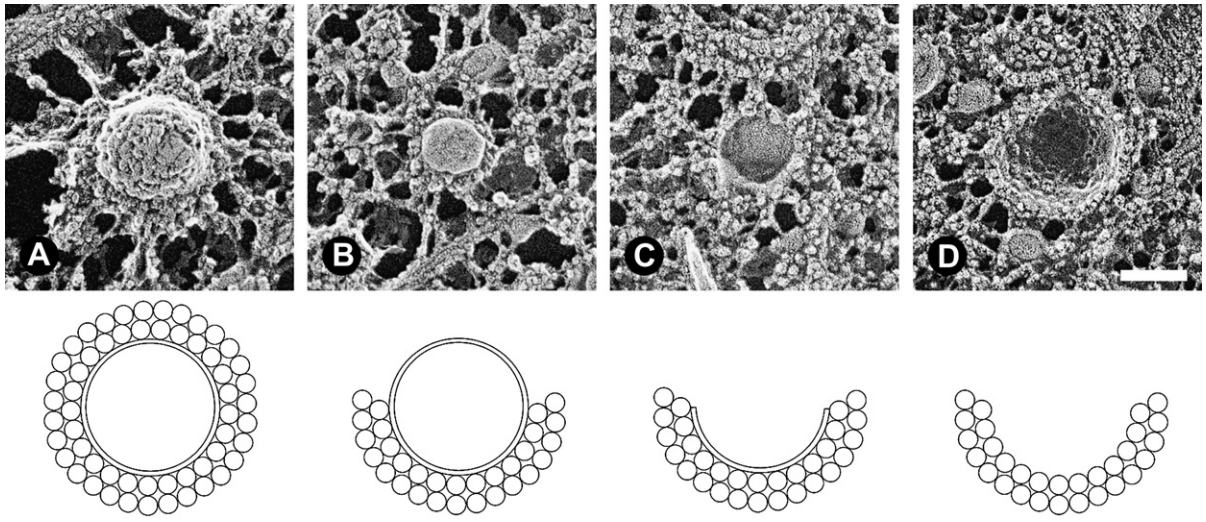

Fig. 6. The ultrastructure of the LLP-SGs complex as revealed by fracturing of four LLPs (34-year-old eye). Under each image is a sketch depicting the observed LLP–SGs complex. (A) A complete complex. Short struts were seen radiating from the complex and associating with other extracellular matrix components. (B) A complex with the upper half of SGs surrounding layers removed. (C) A complex with both the upper SGs and the core of LLP removed. (D) A complex with only the lower half SGs surrounding layers remained. All four conformations of the complex were often observed. Bar 100 nm.

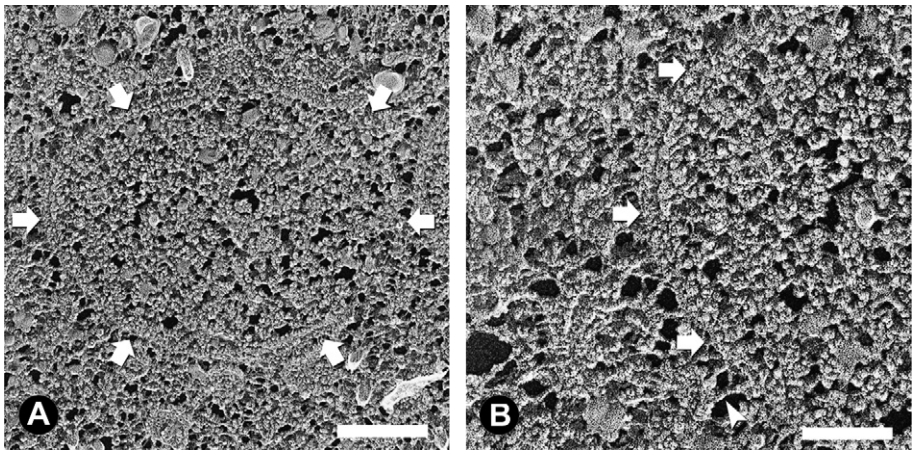

Fig. 7. (A) A CMBB is shown in the center of the image of a 34-year-old eye. Both the LLP and SG could be found within the membrane-like structure (arrows). These components seemed to be associated with each other via thin fibrils. Bar 300 nm. (B) Higher magnification view of the membrane-like structure (arrows). Short struts extended from the membrane and associated with other components in the tissue (arrowhead). Bar 150 nm.

Even in older eyes, this layer was never filled with the significant inclusions in contrast to other layers, particularly the ICL.

The EL was the first layer that appeared filled with a significant amount of LLP and SG inclusions (Fig. 13). Discernible accumulation of inclusions in this layer seemed to begin in eyes >30 years (Fig. 13B). In eyes 40–50 years, the amount of LLP and SG depositions in this layer had increased to the extent that the EL became the most packed region among the middle layers of the tissue (Fig. 13C–E). In spite of the high density of LLP deposition in this area, clusters of LLPs were rarely observed perhaps because there was also a large amount of SG deposition among individual LLPs. The level of the deposition was such that the EL was always filled by LLPs and SGs in eyes >60 years (Fig. 13F–H).

The most extensive age-related changes seen in BrM were seen in and around the ICL. In eye samples <41 years, the layer was nearly deposit-free (Fig. 14A–C). As the donor age increased, more LLPs and SGs became associated with the fine filaments in the ICL, forming groups of inclusions (Fig. 14D). In eyes 50–60 years, this layer began gradually to be filled by the LLPs and SGs. This accumulation appeared to begin from the EL side and extend to the RPE side. In donor eyes >60 years, the ICL was nearly stuffed by these inclusions (Fig. 14E–H). With the ICL packed by LLPs and SGs, patches of LLPs began to develop between the ICL and the BL-RPE and that ultimately resulted in the formation of a lipid wall in eyes >70 years (Ruberti et al., 2003).

Located at the boundary between the BL-RPE and ICL, the lipid wall was a nearly confluent layer composed of LLPs and SGs. Eyes <30 years rarely showed LLP deposition in this area (Fig. 15A). With increased age, the number of inclusions residing at this boundary increased and collagen fibrils connecting the RPE-BL to the ICL became less visible (Fig. 15B–F). A close examination showed that these inclusions seemed to be trapped among the fine fibrils that extended from the lamina densa to collagen in the ICL. Gradually the inclusions filled the interfibrillar spacing and formed patches of particles in eyes >60 years (Fig. 16). With the expanding of the area occupied by these patches, they developed into a thin continuous

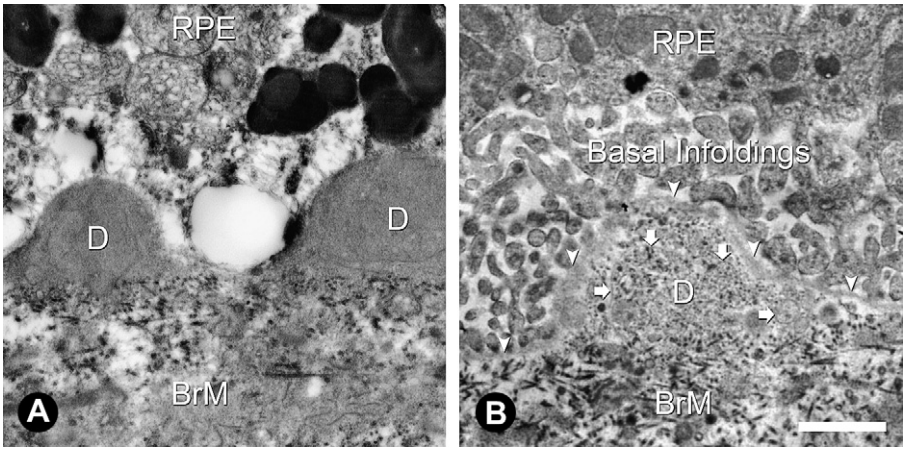

Fig. 8. Drusenoid structures (D) seen in (A) 29- and (B) 50-year-old eyes prepared by OTAP method. CMBBs were present in (B, arrows). Arrowheads, BL-RPE. Bar 1 μm.

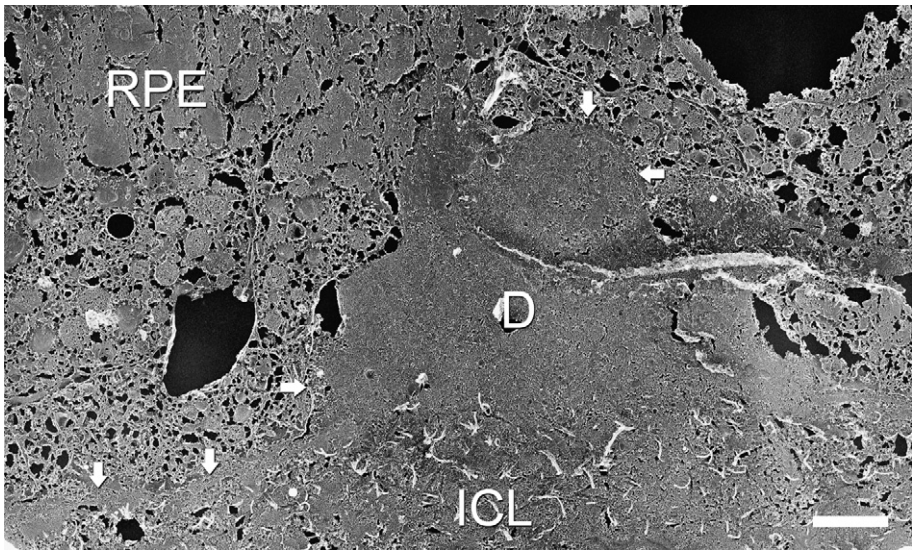

Fig. 9. Drusenoid structure (D) seen in a 59-year-old eye. The dome-shaped deposit was located between the BL-RPE and ICL. Arrows indicate the location of the BL-RPE. Bar 2 μm.

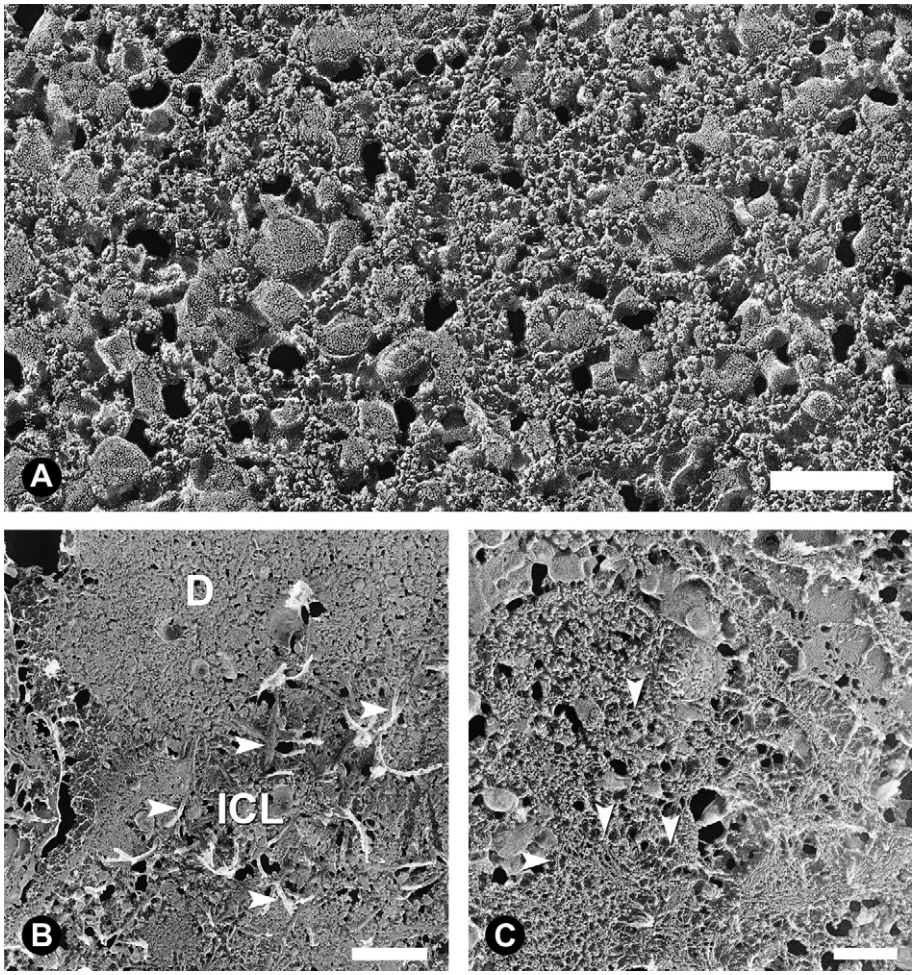

Fig. 10. Higher magnification views of the drusenoid structure in Fig. 9. (A) Components of the drusenoid structure. All three types of inclusions, associated with each other via fine fibrils, were present. CMBBs seemed to be major component of the structure. Bar 200 nm. (B) No collagen fibrils (arrowheads) of the ICL were found within the drusenoid structure (D). Bar 800 nm. (C) Thin fibrils (arrowheads) were seen extended from the BL-RPE into the drusenoid structure. Bar 200 nm.

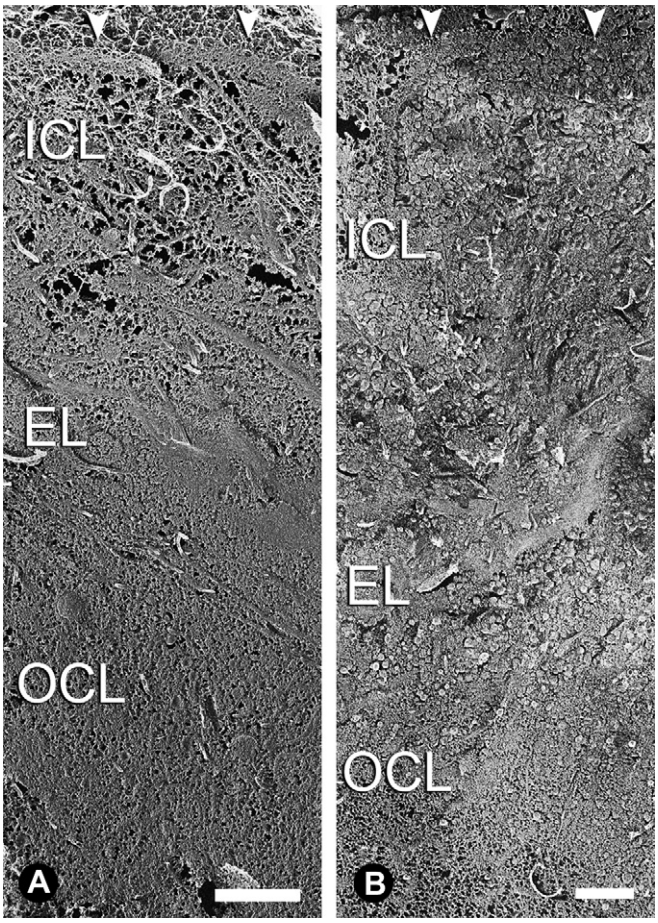

Fig. 11. Oblique sections of BrM of (A) 34- and (B) 77-year-old eyes. Arrowheads indicate the BL-RPE. The EL and OCL of the younger eyes were clearly denser than the ICL. In the older eyes, the EL and ICL were packed with inclusions and thus appeared more crowded than the OCL. Bars 1 μm.

sublayer adjacent to the BL-RPE recognized as the lipid wall (Fig. 16C,F). Unlike other layers filled by both LLPs and SGs, in some old eyes, high magnification images of the sublayer appeared composed mostly of LLPs (Fig. 17). Large and deformed LLPs were usually observed in this tightly packed environment (Fig. 17A).

4. Discussion

In this study, by utilizing both the QFDE and OTAP techniques for sample preparation, we were able to demonstrate ultrastructural features of BrM not easily appreciated using conventional techniques. The limited usage of chemical treatments and ultra-fast slam freezing of the sample tissue of QFDE should have minimized artifacts in our preparations. As diseased eyes were excluded from this study, the results represent a plausible progression of age-related change within BrM.

Our findings are in agreement with other morphological results (Killingsworth, 1987; Marshall et al., 1998) that BrM accumulates a large quantity of variable inclusions during the human lifespan. In addition, the fine preservation of the tissue enabled us to further characterize the components of these inclusions and track their progression in the tissue, with the goal of evaluating the possible impact of these inclusions on the transport through this region.

4.1. Inclusions found in BrM

Several kinds of inclusions had been reported in BrM. Those described by Killingsworth (1987) included coated vesicle-like bodies, electron-lucent droplets, CMBBs, and fibrous banded materials seen in the tissue. In another study, Pauleikhoff et al. (1990) indicated the appearance of small membrane-bound vesicles and membrane fragments. Other studies also reported membranous debris (Curcio and Millican, 1999; Curcio et al., 2005a), long spacing collagens (Sarks, 1976; van der Schaft et al., 1991), drusen (Green and Enger, 1993; Sarks et al., 1999; Hageman and Mullins, 1999)), and fine granules in BrM (Killingsworth, 1987; Curcio and Millican, 1999). In our studies, we found three types of inclusions in QFDE images: LLPs, SGs, and membrane-like structures. However, by combining these different types of inclusions, it appeared that, except for long spacing collagens, all of the different kinds of inclusions mentioned in other studies could be demonstrated in our findings.

One of the most prominent inclusions seen in BrM was the LLPs. These particles were usually 60–80 nm in diameter, with a solid core surrounded by a thin surface layer. Their morphological features were similar to those of the small membrane-bound vesicles, or coated vesicle-like bodies, sometimes called ‘‘electron-lucent particles’’ depending on the morphological technique used for sample preparation (Killingsworth, 1987; Sarks et al., 1988; Curcio and Millican, 1999). The LLPs were usually about 70 nm wide (Killingsworth, 1987; Curcio and Millican, 1999; Ruberti et al., 2003). It was found that the electron-lucent part of this deposit was actually solid and was likely removed during the dehydration process for conventional thin-sectioning TEM preparation (Ruberti et al., 2003; Curcio et al., 2005a). It had been reported that there was another form of the coated vesicle-like bodies that was ‘‘spiked’’ and around 110 nm wide (Killingsworth, 1987). In the current study, we found that the complex composed by single LLP surrounded by SGs, common in all middle layers of BrM, resembled this type of formation.

The small granules were another major deposit found in our study. Morphologically, these were much smaller spheroids than the LLPs. Although they resembled the ‘‘fine granules’’ found using other sample preparation techniques (Killingsworth, 1987), to our knowledge this was the first time the SGs were found to contribute significantly in the inclusion accumulation in BrM. The identity of these small particles remains to be determined. However, our finding of the complex formed by the SGs and single LLP suggests a possible interaction between these two inclusion types.

The coated membrane-bound body (CMBB) was a major deposit described in other morphological studies (Killingsworth, 1987; Marshall et al., 1998). It was characterized as a membrane-bound substructure with fine granules, electron-lucent particles, and coated vesicle-like bodies inside (Killingsworth,

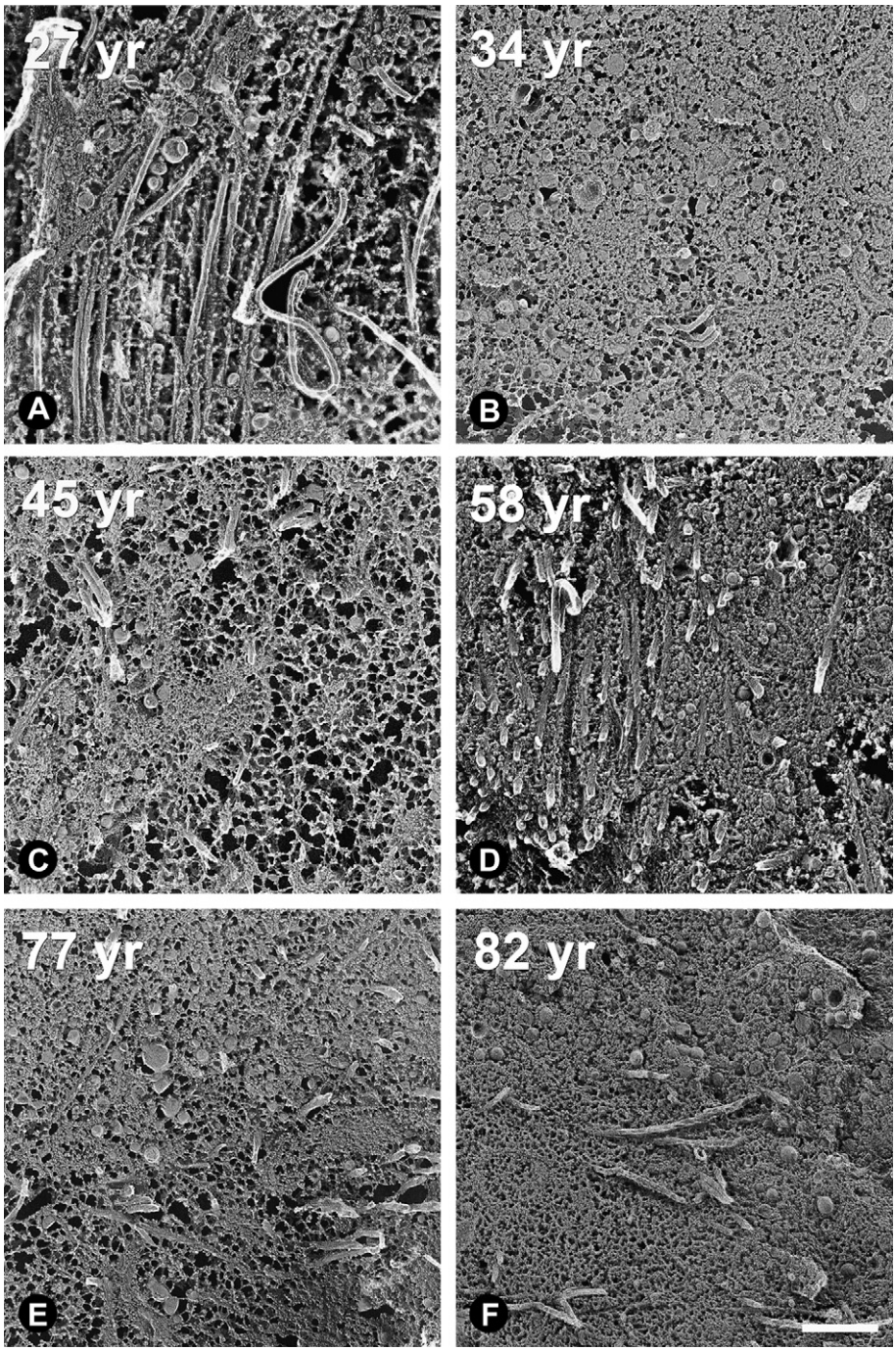

Fig. 12. Age-related changes of OCL. The inclusions did not seem to fill the interfibrillar spacing of the OCL. Images of younger eyes as shown in (A) to (C) resembled older ones as (D) to (F). Bar 500 nm.

1987). Our findings confirmed this ultrastructure as the QFDE images showing CMBBs were composed of the membrane-like structures surrounding LLPs and SGs. It had been suggested the membrane-like structures were lipid-rich (Curcio et al., 2001), and their association with other matrix materials via short struts implied a probable binding mechanism of the CMBB in the tissue.

As only one drusenoid structure was observed in QFDE preparation of our study, its morphological features could not represent all types of drusen described in other studies (Green et al., 1985; Green and Enger, 1993; Sarks et al., 1999; Hageman and Mullins, 1999). Nevertheless it fits the characteristics of an ''entrapment site'', a phenotype of CMBBs described in eyes with clinically undetectable drusen (Sarks et al., 1999). It has been suggested that the formation of the drusen is caused by CMBBs unable to penetrate the tightly woven collagens of the ICL (Sarks et al., 1999). However, our findings of CMBBs in all three middle layers of BrM indicated either the CMBBs were mobile in spite of their relatively large size, or that this type of inclusion was formed locally via some unknown mechanism.

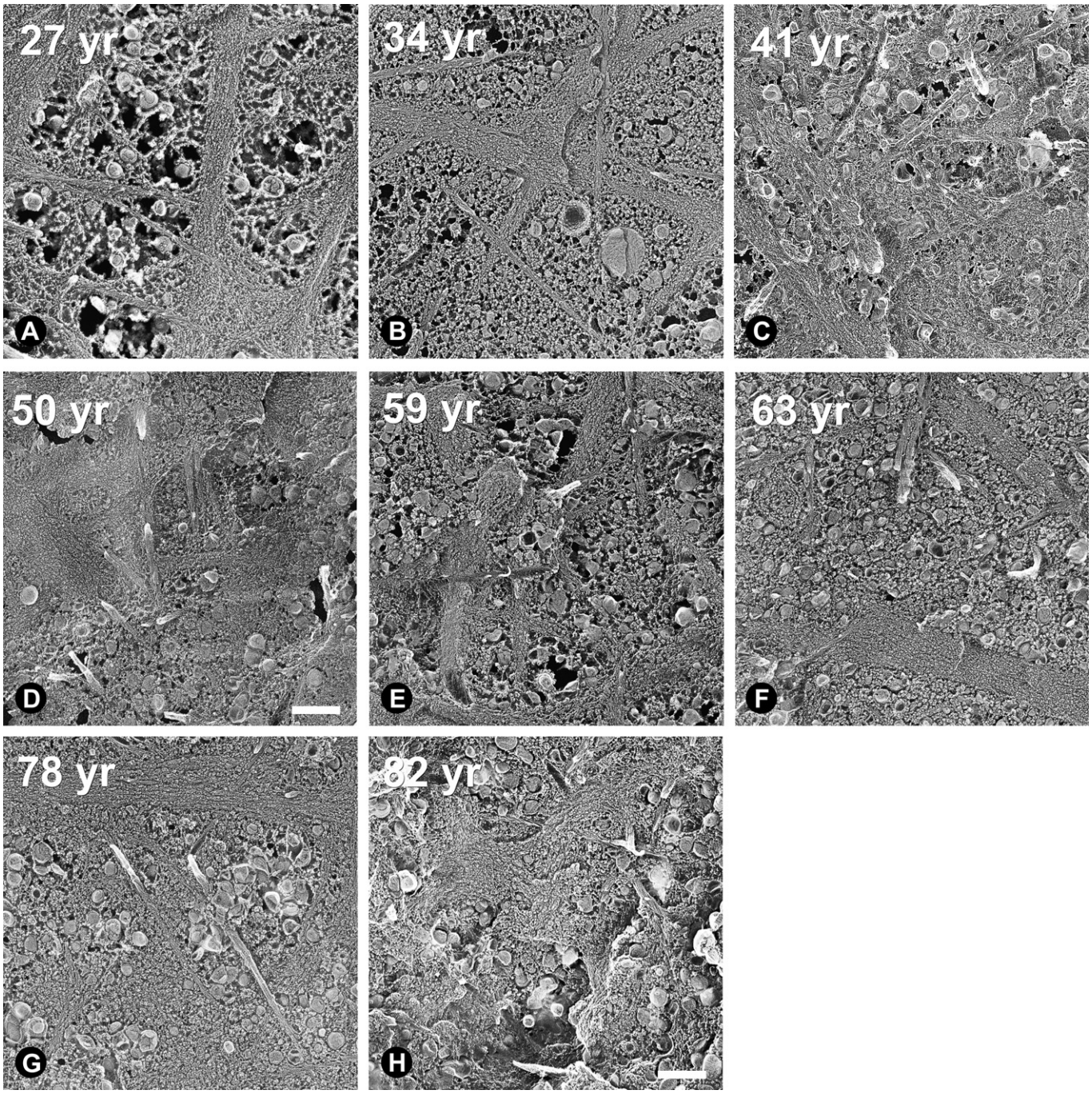

Fig. 13. Age-related changes of EL. Eyes >34 years were packed with inclusions in this layer. Bar 300 nm.

The only deposit type seen in BrM that we did not identify in the QFDE images was the long spacing collagen. We were able to see such inclusions in our OTAP thin-sectioning TEM examination. The long spacing collagen has been described as parallel banded collagen-like materials with an axial periodicity about 100 nm (Killingsworth, 1987; Knupp et al., 2002). We suspected those structures were not easily identified in our QFDE images due to the inability to preserve the periodic banding of collagen fibrils when using this technique. We found that although the high magnification QFDE images were capable of characterizing the collagen fibrils as composed by coiled microfibrils, they rarely showed the 64 nm axial banding that was usually apparent in other studies (Marshall et al., 1998). This banding has been seen using heavy metal staining (Hodge and Schmitt, 1960; Meek et al., 1979), typical of conventional preparation, which is not part of specimen preparation by QFDE.

4.2. Possible mechanism of LLP accumulation

We found significant age-related accumulation of LLPs in BrM. In high magnification QFDE images, it appeared that the inclusions we saw were frequently in contact with collagen

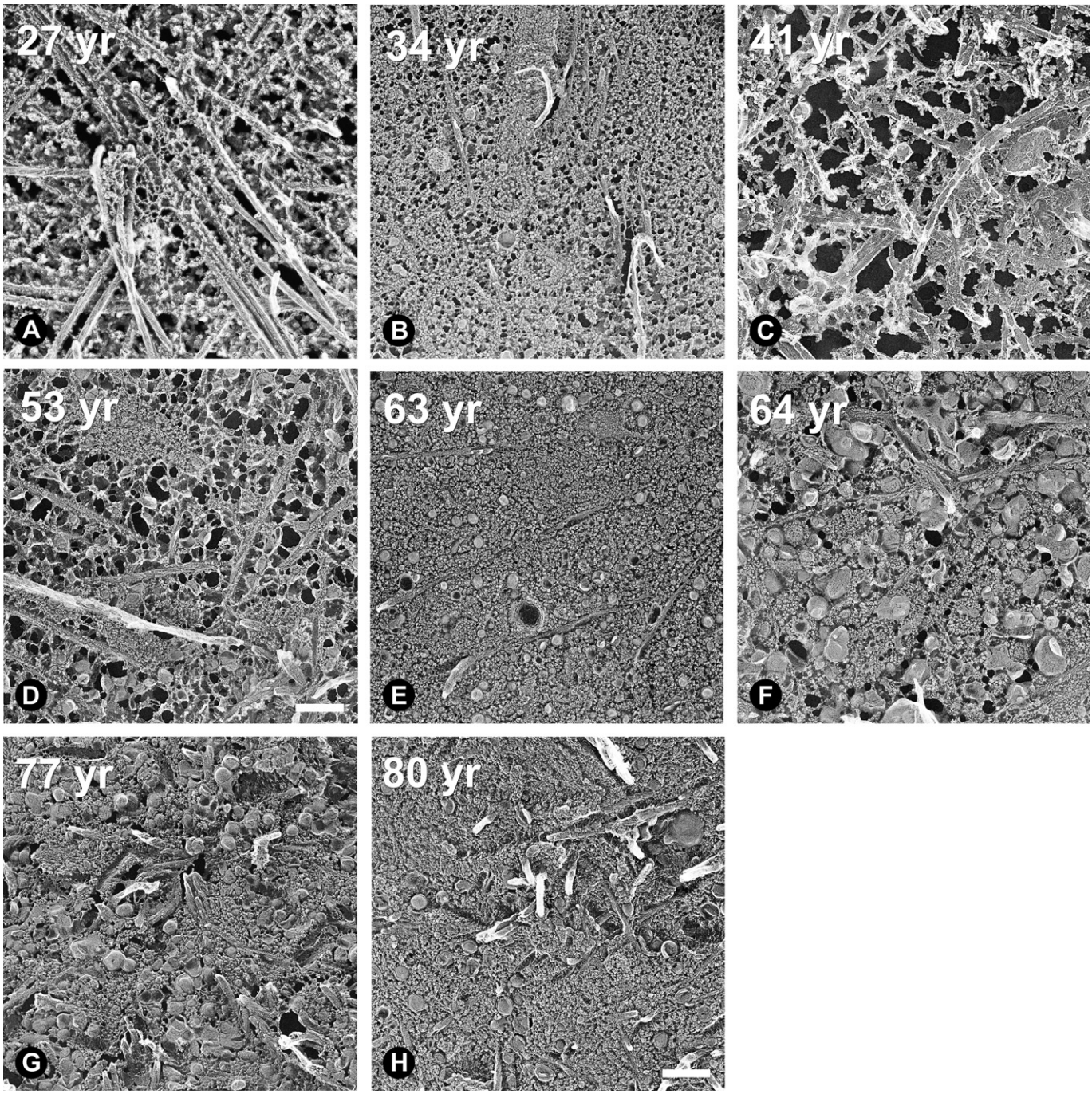

Fig. 14. Age-related changes of ICL. Eyes >60 years were packed with inclusions in this layer. Bar 300 nm.

or elastic fibrils by fine filaments that resembled proteoglycans. One possible mechanism of accumulation could be the embedding of the LLPs in the fibrils either due to higher filament density in that region (Starita et al., 1997) or increased cross-linking of fibrils (Karwatowski et al., 1995; Handa et al., 1999). The recent discovery of potential apolipoprotein B-100 (ApoB-100) on the LLPs (Li et al., 2005a, 2006) suggests that this attachment might be similar to the mechanism causing low density lipoprotein (LDL) accumulation in the vascular intima. It has been postulated that LDL accumulation in vascular intima is initiated by the ApoB-100 interacting with the sulfate groups of the proteoglycans and further promoted by the oxidative modification of LDL (Williams and Tabas, 1995; Chang et al., 2001; Wang et al., 2001; Skalen et al., 2002; Stocker and Keaney, 2004; Vijayagopal and Menon, 2005). Considering that the biochemical and ultrastructural environments of BrM and vascular intima are similar (Curcio et al., 2001; Sivaprasad et al., 2005), this mechanism may also apply to the LLP retention observed in our study.

Our findings indicate that the EL was the first layer that was filled by LLPs and SGs. This may be analogous to the early pathogenesis of an arteriosclerosis that demonstrates LDL

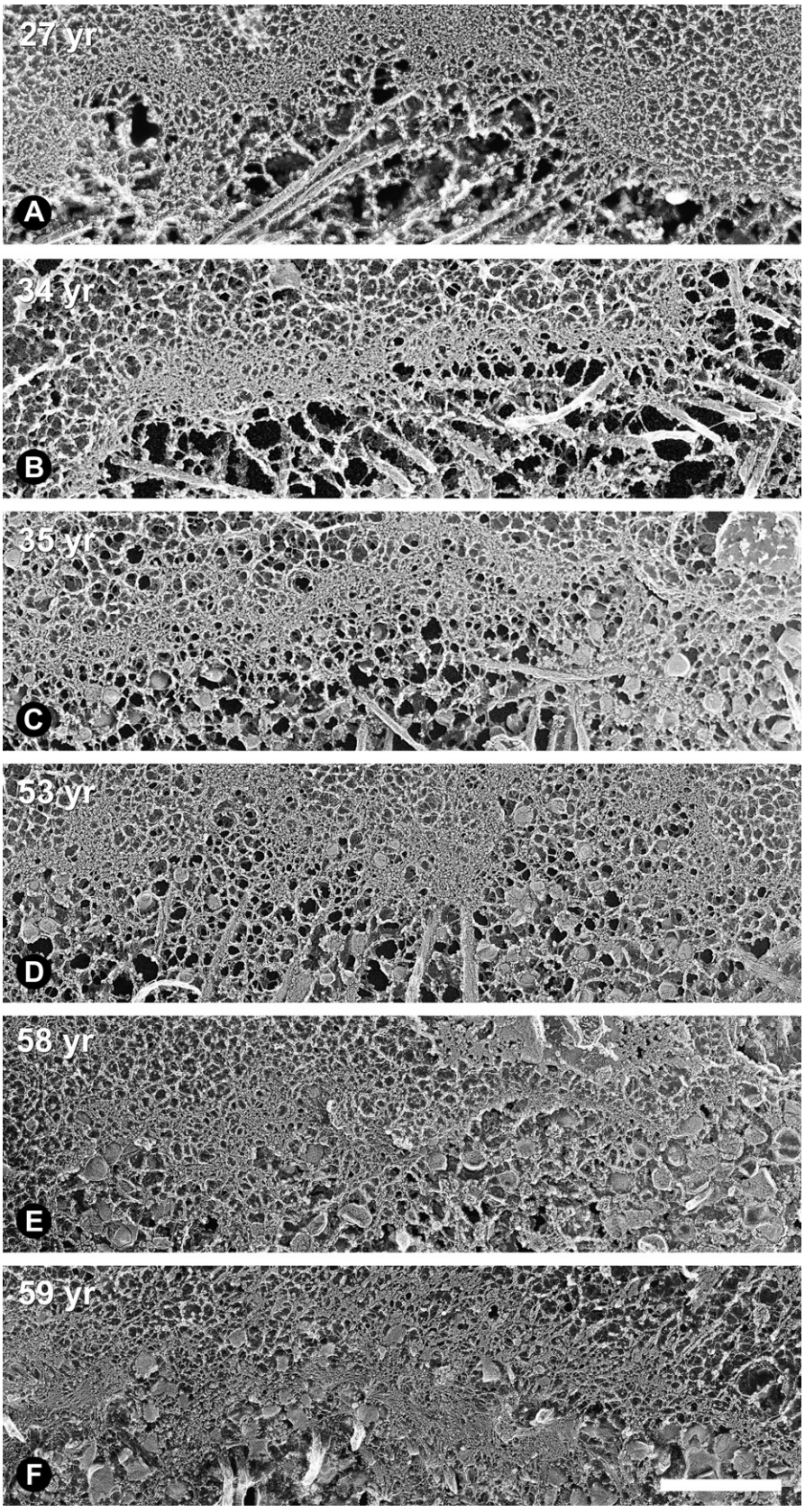

Fig. 15. Age-related changes of the boundary between the BL-RPE and ICL in eyes <60 years. The lamina lucida and lamina densa of the BL-RPE can be clearly distinguished as the former has much more interfibrillar spacing. Bar 500 nm.

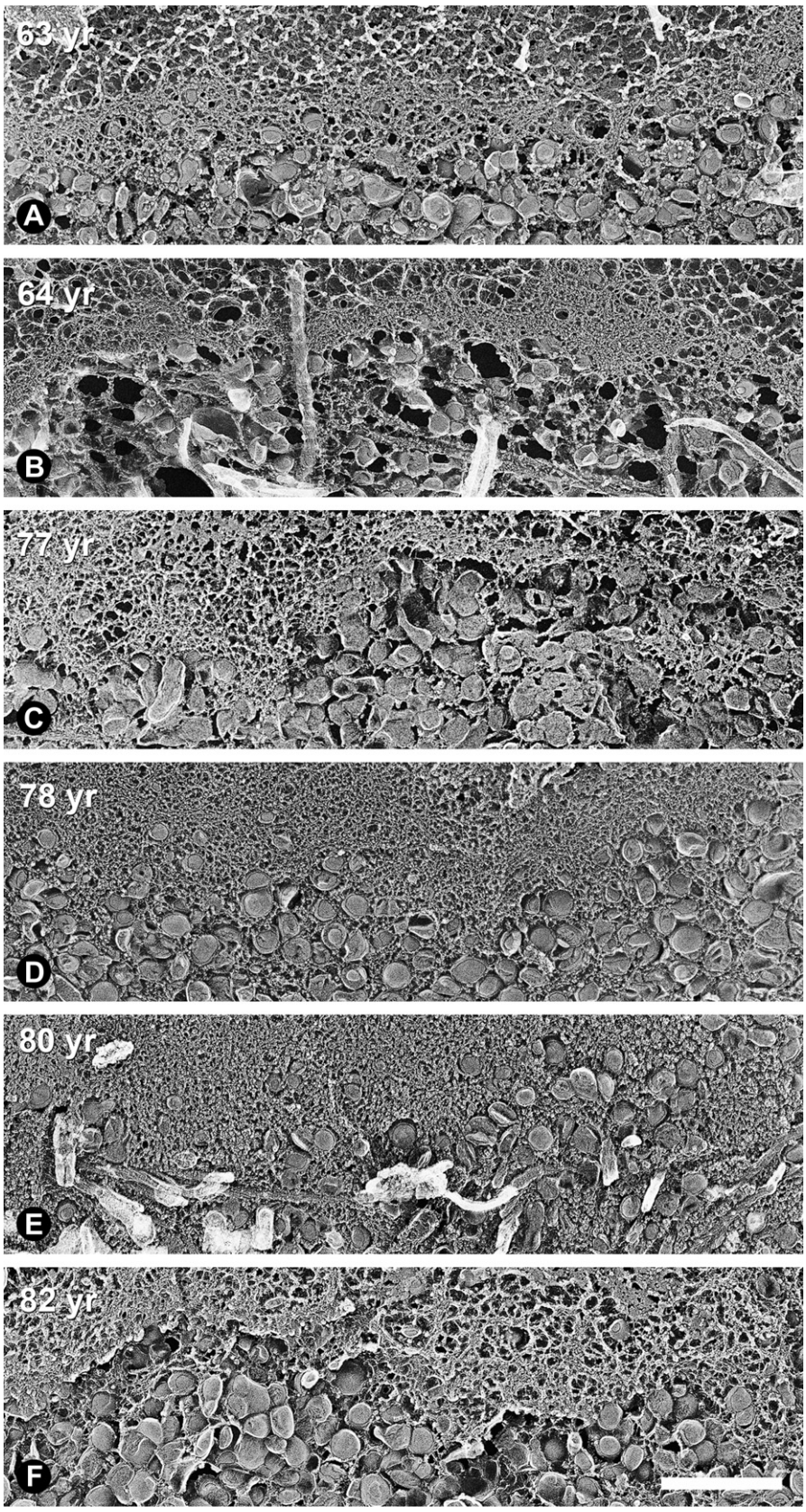

Fig. 16. The formation of lipid walls in older eyes. Patches of the lipid wall were seen in the boundary between the BL-RPE and ICL in eyes >60 years. It appeared that the lipid wall formed at different ages for different eyes. The lipid wall was found in some eyes such as (C) and (F), while in others (D,E) fewer LLPs were observed. Bar 500 nm.

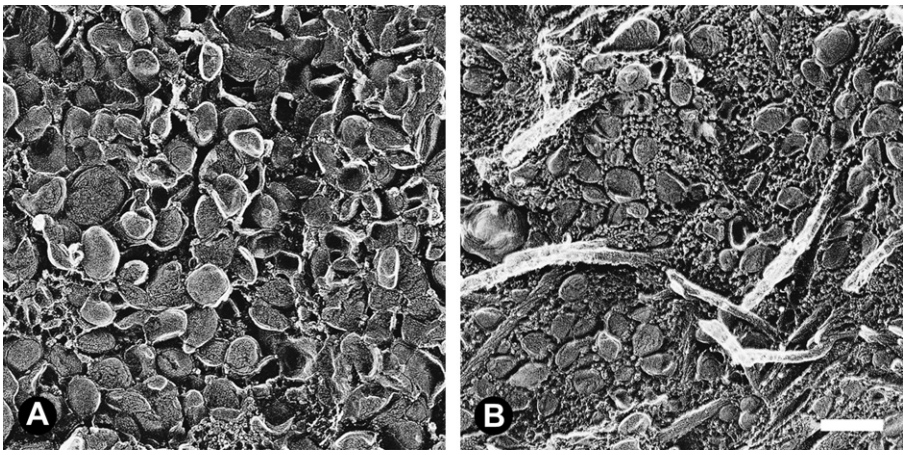

Fig. 17. Comparison between the ultrastructure of the (A) lipid wall and (B) inclusions in the ICL of an 82-year-old eye. The lipid wall of this eye was mainly composed of tightly packed LLPs, while both the SGs and LLPs filled interfibrillar spacing in the ICL. Large and deformed LLPs were usually seen in the lipid wall. Bar 200 nm.

depositions in the elastic lamina of the vascular intima (Kramsch and Hollander, 1973; Guyton et al., 1985; Bocan et al., 1988; Podet et al., 1991; Bobryshev and Lord, 1999; Wang et al, 2001). It has been postulated that LDLs can interact with elastin fibrils via hydrophobic amino acids (Bobryshev and Lord, 1999) or by interactions between the oxidized LDL and calcium ion binding elastin fibrils (Wang et al., 2001). It remains to be determined if these mechanisms apply to the LLP deposition in the EL of BrM.

In addition to the accumulation mechanisms mentioned above, a further factor that may lead to LLP accumulation is likely the low void space within the EL. As we compared the EL with the ICL in young eyes, it appeared the EL contained more extracellular materials. Hence the EL will be filled faster than the ICL, given similar mechanisms at work in both layers.

4.3. What is the origin of the LLPs?

There are a variety of theories regarding the source of the LLPs found in BrM (Holz et al., 1994; Mullins et al., 2000; Curcio et al., 2001, 2005a; Li et al., 2005a; Sivaprasad et al., 2005). One potential source of these inclusions is the plasma LDLs entering from the choriocapillaris, as the morphological features of LLPs are similar to aggregated LDLs found in vascular intima (Frank and Fogelman, 1989). It has been reported that plasma LDLs are transported from choriocapillaris into RPE cells (Gordiyenko et al., 2004). Alternatively, the recent findings that mRNA for both apoB and microsomal triglyceride transfer protein, necessary for lipoprotein assembly, are located within RPE cells (Malek et al., 2003; Li et al., 2005b), and that there are significant differences in the density profile and cholesterol distribution of LLPs and plasma lipoproteins (Li et al., 2005a) suggest that RPE cells package LLPs as a new type of lipoprotein particle which then translocates through BrM (Curcio et al., 2005b).

The morphological findings of this study are not conclusive on this issue. The early LLP accumulations in the OCL could be consistent with a plasma origin of these inclusions. However, our finding that accumulation of LLPs progressively filled the EL and ICL while the OCL remained relatively open implies that the RPE-originated particles are impeded by the barrier in the middle of BrM and thus accumulate in the inner aspect of the tissue. The formation of the lipid wall only after the EL and ICL are filled by inclusions also suggests that LLPs squeezing through the BL-RPE are blocked by the filled ICL thus leading them to aggregate between the ICL and BL-RPE. It seems unlikely that LLPs can penetrate a thick barrier in the middle of BrM in old eyes to form the lipid wall if they arrive via a vascular source.

The mechanism of transport of the LLPs from RPE to choroid has yet to be determined. The average size of LLPs appears larger than the interfibrillar spacing of the lamina densa in the BL-RPE. Hence, whether they can pass through this tight network remains questionable. One possible explanation is that smaller particles pass through the lamina and fuse together to form larger LLPs. Another possibility is that particles and/or the lamina densa deform to allow the LLPs to squeeze through, as suggested in the study of the transport of chylomicrons through the basal lamina into lymphatic channels (Sabesin and Frase, 1977). A future study evaluating the size distribution of LLPs seen in BrM utilizing the QFDE images is warranted.

5. Conclusions

Grindle and Marshall (1978) proposed that a hydrophobic barrier in BrM could compromise the transport between RPE cells and choroids and this could lead to RPE detachments. In the current study, the QFDE and OTAP techniques applied to the examination of the age-related changes in BrM provided a detailed characterization of age-related changes in the ultrastructure of the components of the tissue. Our findings not only confirmed several types of inclusions demonstrated by other morphological studies but also further suggested that three basic kinds of inclusions could participate in different combinations. We found that the LLPs were not the only inclusions collected in the tissue. The SGs also contributed significantly to this

accumulation. The identity of these latter particles was unclear. In addition, the associations between these inclusions and fine filaments in the tissue implied probable interactions between these components that might account for the accumulation of inclusions. The progressive filling by inclusions in the EL and ICL of BrM and the formation of the lipid wall would probably result in the decrease of the hydraulic conductivity as described in other studies (Moore et al., 1995; Starita et al., 1996).

Acknowledgements

We would like to thank Dr Jeffery W. Ruberti for technical assistance. This study is supported by NIH EY014662, NIH EY06109, and The American Health Assistance Foundation.

References

Anderson, D.H., Fisher, S.K., Steinberg, R.H., 1978. Mammalian cones: disc shedding, phagocytosis, and renewal. Invest. Ophthalmol. Vis. Sci. 17, 117–133.

Bird, A.C., Marshall, J., 1986. Retinal pigment epithelial detachments in the elderly. Trans. Ophthalmol. Soc. UK 105, 674–682.

Bobryshev, Y.V., Lord, R.S., 1999. Accumulation of co-localised unesterified cholesterol and neutral lipids within vacuolised elastin fibres in atheroprone areas of the human aorta. Atherosclerosis 142, 121–131.

Bocan, T.M., Brown, S.A., Guyton, J.R., 1988. Human aortic fibrolipid lesions. Immunochemical localization of apolipoprotein B and apolipoprotein A. Arteriosclerosis 8, 499–508.

Chang, M.Y., Potter-Perigo, S., Wight, T.N., Chait, A., 2001. Oxidized LDL bind to nonproteoglycan components of smooth muscle extracellular matrices. J. Lipid Res. 42, 824–833.

Chen, J.C., Fitzke, F.W., Pauleikhoff, D., Bird, A.C., 1992. Functional loss in age-related Bruch's membrane change with choroidal perfusion defect. Invest. Ophthalmol. Vis. Sci. 33, 334–340.

Curcio, C.A., Millican, C.L., 1999. Basal linear deposit and large drusen are specific for early age-related maculopathy. Arch. Ophthalmol. 117, 329–339.

Curcio, C.A., Millican, C.L., Bailey, T., Kruth, H.S., 2001. Accumulation of cholesterol with age in human Bruch's membrane. Invest. Ophthalmol. Vis. Sci. 42, 265–274.

Curcio, C.A., Presley, J.B., Millican, C.L., Medeiros, N.E., 2005a. Basal deposits and drusen in eyes with age-related maculopathy: evidence for solid lipid particles. Exp. Eye Res. 80, 761–775.

Curcio, C.A., Presley, J.B., Malek, G., Medeiros, N.E., Avery, D.V., Kruth, H.S., 2005b. Esterified and unesterified cholesterol in drusen and basal deposits of eyes with age-related maculopathy. Exp. Eye Res. 81, 731–741.

Feeney-Burns, L., Ellersieck, M.R., 1985. Age-related changes in the ultrastructure of Bruch's membrane. Am. J. Ophthalmol. 15, 686–697.

Foster, A., Resnikoff, S., 2005. The impact of Vision 2020 on global blindness. Eye 19, 1133–1135.

Frank, J.S., Fogelman, A.M., 1989. Ultrastructure of the intima in WHHL and cholesterol-fed rabbit aortas prepared by ultra-rapid freezing and freeze-etching. J. Lipid Res. 30, 967–978.

Giusto, N.M., Castagnet, P.I., Ilincheta, M.G., Roque, M.E., Pasquare, S.J., 1997. Lipid metabolism in photoreceptor membranes: regulation and mechanisms. Neurochem. Res. 22, 445–453.

Gordiyenko, N., Campos, M., Lee, J.W., Fariss, R.N., Sztein, J., Rodriguez, I.R., 2004. RPE cells internalize low-density lipoprotein (LDL) and oxidized LDL (oxLDL) in large quantities in vitro and in vivo. Invest. Ophthalmol. Vis. Sci. 45, 2822–2829.

Green, W.R., Enger, C., 1993. Age-related macular degeneration histopathologic studies. The 1992 Lorenz E. Zimmerman Lecture. Ophthalmology 100, 1519–1535.

Green, W.R., McDonnell, P.J., Yeo, J.H., 1985. Pathologic features of senile macular degeneration. Ophthalmology 92, 615–627.

Grindle, C.F., Marshall, J., 1978. Ageing changes in Bruch's membrane and their functional implications. Trans. Ophthalmol. Soc. UK 98, 172–175.

Guyton, J.R., Klemp, K.F., 1988. Ultrastructural discrimination of lipid droplets and vesicles in atherosclerosis: value of osmium-thiocarbohydrazide-osmium and tannic acid-paraphenylenediamine techniques. J. Histochem. Cytochem. 36, 1319–1328.

Guyton, J.R., Bocan, T.M., Schifani, T.A., 1985. Quantitative ultrastructural analysis of perifibrous lipid and its association with elastin in nonatherosclerotic human aorta. Arteriosclerosis 5, 644–652.

Hageman, G.S., Mullins, R.F., 1999. Molecular composition of drusen as related to substructural phenotype. Mol. Vis. 5, 28.

Handa, J.T., Verzijl, N., Matsunaga, H., Aotaki-Keen, A., Lutty, G.A., te Koppele, J.M., Miyata, T., Hjelmeland, L.M., 1999. Increase in the advanced glycation end product pentosidine in Bruch's membrane with age. Invest. Ophthalmol. Vis. Sci. 40, 775–779.

Hodge, A.J., Schmitt, F.O., 1960. The charge profile of the tropocollagen macromolecule and the packing arrangement in native-type collagen fibrils. Proc. Natl. Acad. Sci. 46, 186–197.

Hogan, M.J., Alvarado, J., 1967. Studies on the human macula. IV. Aging changes in Bruch's membrane. Arch. Ophthalmol. 77, 410–420.

Holz, F.G., Sheraidah, G., Pauleikhoff, D., Bird, A.C., 1994. Analysis of lipid deposits extracted from human macular and peripheral Bruch's membrane. Arch. Ophthalmol. 112, 402–406.

Huang, J.-D., 2007. Characterization of age-related accumulations of lipid particles in Bruch's membrane. PhD thesis. Northwestern University, Evanston, IL.

Hussain, A.A., Rowe, L., Marshall, J., 2002. Age-related alternations in the diffusional transport of amino acids across the human Bruch's-choroid complex. J. Opt. Soc. Am. 19, 166–172.

Karwatowski, W.S., Jeffries, T.E., Duance, V.C., Albon, J., Bailey, A.J., Easty, D.L., 1995. Preparation of Bruch's membrane and analysis of the age-related changes in the structural collagens. Br. J. Ophthalmol. 79, 944–952.

Killingsworth, M.C., 1987. Age-related components of Bruch's membrane in the human eye. Graefe's Arch. Clin. Exp. Ophthalmol. 225, 406–412.

Knupp, C., Amin, S.Z., Munro, P.M., Luthert, P.J., Squire, J.M., 2002. Collagen VI assemblies in age-related macular degeneration. J. Struct. Biol. 139, 181–189.

Kornzweig, A.L., 1977. Changes in the choriocapillaris associated with senile macular degeneration. Ann. Ophthalmol. 9, 753–762.

Korte, G.E., Burns, M.S., Bellhorn, R.W., 1989. Epithelium-capillary interactions in the eye: the retinal pigment epithelium and the choriocapillaris. Int. Rev. Cytol. 114, 221–248.

Kramsch, D.M., Hollander, W., 1973. The interaction of serum and arterial lipoproteins with elastin of the arterial intima and its role in the lipid accumulation in atherosclerotic plaques. J. Clin. Invest. 52, 236–247.

Li, C.M., Chung, B.H., Presley, J.B., Malek, G., Zhang, X., Dashti, N., Li, L., Chen, J., Bradley, K., Kruth, H.S., Curcio, C.A., 2005a. Lipoprotein-like particles and cholesteryl esters in human Bruch's membrane: initial characterization. Invest. Ophthalmol. Vis. Sci. 46, 2576–2586.

Li, C.M., Presley, J.B., Zhang, X., Dashti, N., Chung, B.H., Medeiros, N.E., Guidry, C., Curcio, C.A., 2005b. Retina expresses microsomal triglyceride transfer protein: implications for age-related maculopathy. J Lipid Res. 46, 628–640.

Li, C.M., Clark, M.E., Chimento, M.F., Curcio, C.A., 2006. Apolipoprotein localization in isolated drusen and retinal apolipoprotein gene expression. Invest. Ophthalmol. Vis. Sci. 47, 3119–3128.

Malek, G., Li, C.M., Guidry, C., Medeiros, N.E., Curcio, C.A., 2003. Apolipoprotein B in cholesterol-containing drusen and basal deposits of human eyes with age-related maculopathy. Am. J. Pathol. 162, 413–425.

Marshall, J., Hussain, A.A., Starita, C., Moore, D.J., Patmore, A.L., 1998. Ageing and Bruch's membrane. In: Marmor, M.F., Wolfensberget, T.J. (Eds.), Retinal Pigment Epithelium: Function and Disease. Oxford University Press, New York, pp. 669–692.

Matsumoto, B., Defoe, D.M., Besharse, J.C., 1987. Membrane turnover in rod photoreceptors: ensheathment and phagocytosis of outer segment distal tips by pseudopodia of the retinal pigment epithelium. Proc. R. Soc. Lond. B. Biol. Sci. 230, 339–354.

Meek, K.M., Chapman, J.A., Hardcastle, R.A., 1979. The staining pattern of collagen fibrils. Improved correlation with sequence data. J. Biol. Chem. 254, 10710–10714.

Moore, D.J., Hussain, A.A., Marshall, J., 1995. Age-related variation in the hydraulic conductivity of Bruch's membrane. Invest. Ophthalmol. Vis. Sci. 36, 1290–1297.

Mullins, R.F., Russell, S.R., Anderson, D.H., Hageman, G.S., 2000. Drusen associated with aging and age-related macular degeneration contain proteins common to extracellular deposits associated with atherosclerosis, elastosis, amyloidosis, and dense deposit disease. FASEB J. 14, 835–846.

Nakaizumi, Y., Hogan, M.J., Feeney, L., 1964. The ultrastructure of Bruch's membrane. 3. The macular area of the human eye. Arch. Ophthalmol. 72, 395–400.

Newsome, D.A., Huh, W., Green, W.R., 1987. Bruch's membrane age-related changes vary by region. Curr. Eye Res. 6, 1211–1221.

Overby, D., Ruberti, J., Gong, H., Freddo, T.F., Johnson, M., 2001. Specific hydraulic conductivity of corneal stroma as seen by quick-freeze/deep-etch. J. Biomech. Eng. 123, 154–161.

Pauleikhoff, D., Barondes, M.J., Minassian, D., Chisholm, I.H., Bird, A.C., 1990. Drusen as risk factors in age-related macular disease. Am. J. Ophthalmol. 109, 38–43.

Podet, E.J., Shaffer, D.R., Gianturco, S.H., Bradley, W.A., Yang, C.Y., Guyton, J.R., 1991. Interaction of low density lipoproteins with human aortic elastin. Arterioscler. Thromb. 11, 116–122.

Ramrattan, R.S., van der Schaft, T.L., Mooy, C.M., de Bruijn, W.C., Mulder, P.G., de Jong, P.T., 1994. Morphometric analysis of Bruch's membrane, the choriocapillaris, and the choroid in aging. Invest. Ophthalmol. Vis. Sci. 35, 2857–2864.

Ruberti, J.W., Curcio, C.A., Millican, C.L., Menco, B.P., Huang, J.D., Johnson, M., 2003. Quick-freeze/deep-etch visualization of age-related lipid accumulation in Bruch's membrane. Invest. Ophthalmol. Vis. Sci. 44, 1753–1759.

Sabesin, S.M., Frase, S., 1977. Electron microscopic studies of the assembly, intracellular transport, and secretion of chylomicrons by rat intestine. J. Lipid Res. 18, 496–511.

Sarks, J.P., Sarks, S.H., Killingsworth, M.C., 1988. Evolution of geographic atrophy of the retinal pigment epithelium. Eye 2, 552–577.

Sarks, S.H., 1976. Ageing and degeneration in the macular region: a clinico-pathological study. Br. J. Ophthalmol. 60, 324–341.

Sarks, S.H., Arnold, J.J., Killingsworth, M.C., Sarks, J.P., 1999. Early drusen formation in the normal and aging eye and their relation to age related maculopathy: a clinicopathological study. Br. J. Ophthalmol. 83, 358–368.

Sivaprasad, S., Bailey, T.A., Chong, V.N., 2005. Bruch's membrane and the vascular intima: is there a common basis for age-related changes and disease? Clin. Exp. Ophthalmol. 33, 518–523.

Skalen, K., Gustafsson, M., Rydberg, E.K., Hulten, L.M., Wiklund, O., Innerarity, T.L., Boren, J., 2002. Subendothelial retention of atherogenic lipoproteins in early atherosclerosis. Nature 417, 750–754.

Starita, C., Hussain, A.A., Pagliarini, S., Marshall, J., 1996. Hydrodynamics of aging Bruch's membrane: implications for macular disease. Exp. Eye Res. 62, 565–572.

Starita, C., Hussain, A.A., Patmore, A., Marshall, J., 1997. Localization of the site of major resistance to fluid transport in Bruch's membrane. Invest. Ophthalmol. Vis. Sci. 38, 762–767.

Stocker, R., Keaney Jr., J.F., 2004. Role of oxidative modifications in atherosclerosis. Physiol. Rev. 84, 1381–1478.

Ugarte, M., Hussain, A.A., Marshall, J., 2006. An experimental study of the elastic properties of the human Bruch's membrane-choroid complex: relevance to ageing. Br. J. Ophthalmol. 90, 621–626.

van der Schaft, T.L., de Bruijn, W.C., Mooy, C.M., Ketelaars, D.A., de Jong, P.T., 1991. Is basal laminar deposit unique for age-related macular degeneration? Arch. Ophthalmol. 109, 420–425.

van der Schaft, T.L., Mooy, C.M., de Bruijn, W.C., Oron, F.G., Mulder, P.G., de Jong, P.T., 1992. Histologic features of the early stages of age-related macular degeneration. A statistical analysis. Ophthalmology 99, 278–286.

Vijayagopal, P., Menon, P.V., 2005. Varied low density lipoprotein binding property of proteoglycans synthesized by vascular smooth muscle cells cultured on extracellular matrix. Atherosclerosis 178, 75–82.

Wang, X., Greilberger, J., Ratschek, M., Jurgens, G., 2001. Oxidative modifications of LDL increase its binding to extracellular matrix from human aortic intima: influence of lesion development, lipoprotein lipase and calcium. J. Pathol. 195, 244–250.

Williams, K.J., Tabas, I., 1995. The response-to-retention hypothesis of early atherogenesis. Arterioscler. Thromb. Vasc. Biol. 15, 551–561.

Yamada, Y., Ishibashi, K., Ishibashi, K., Bhutto, I.A., Tian, J., Lutty, G.A., Handa, J.T., 2006. The expression of advanced glycation endproduct receptors in rpe cells associated with basal deposits in human maculas. Exp. Eye Res. 82, 840–848.